IMAGE-BASED STATE MODELING OF THE LAND MOBILE SATELLITE CHANNEL FOR MULTI-SATELLITE RECEPTION

Marie Rieche[1], Daniel Arndt[1], Alexander Ihlow[1], Markus Landmann[2], and Giovanni Del Galdo[1]

[1]*Ilmenau University of Technology, Digital Broadcasting Research Lab, Helmholtzplatz 2, 98693 Ilmenau, Germany, name.lastname@tu-ilmenau.de*

[2]*Fraunhofer Institute for Integrated Circuits IIS, Am Wolfsmantel 33, 91058 Erlangen, Germany, markus.landmann@iis.fraunhofer.de*

ABSTRACT

This paper investigates the image-based characterization of the land mobile satellite (LMS) channel. For a comprehensive multi-satellite model, a traditional measurement-based approach is not feasible due to the lack of available satellites at all possible orbital positions and the drawbacks of the measurement system when a high gain tracking antenna is involved (e.g. Ka/Ku band). To overcome these challenges, we propose to derive the LMS channel state-model from an evaluation of hemispheric images of the environment. With geometric considerations we can predict the position of an arbitrary satellite within the image. Based on this information the reception state of the LMS channel can be extracted. We determine the accuracy of our method by comparing it with results from RF (Radio Frequency) measurements.
This image-based approach establishes the basis of propagation modeling even for multi-/single-satellite systems not yet in orbit.

Key words: propagation; channel modeling; land mobile satellite channel; measurements; image processing.

1. INTRODUCTION

Direct-to-home stationary satellite broadcasting as well as bi-directional satellite communication via very small aperture terminals (VSAT) are nowadays of everyday use. Satellite broadcasting systems employing mobile receivers are also increasingly popular. An example is the Satellite Digital Audio Radio Service (SDARS) in the U.S., operated by Sirius XM Radio [1, 2]. Establishing such systems is of high economic risk and needs thorough network planning to meet the customers quality of service (QoS) requirements. Therefore, an adequate description of the underlying radio propagation channel is essential.

Since the 1980s, statistical models for the land mobile satellite (LMS) link are under consideration and have been refined by several measurement campaigns in various environments [3, 4, 5, 6]. These models are based on a characterization of the signal power variations, as depicted in Figure 1. The characterization of the LMS channel on the basis of a sequence of reception states is widely accepted. In the literature, several statistical LMS models incorporating three states (line-of-sight, shadowing, blockage) [7]. Available 2-state-models ([8, 9]) are describing the channel as either *good*(*LoS/ light shadowing*) or *bad*(*NLoS/ heavy shadowing*).

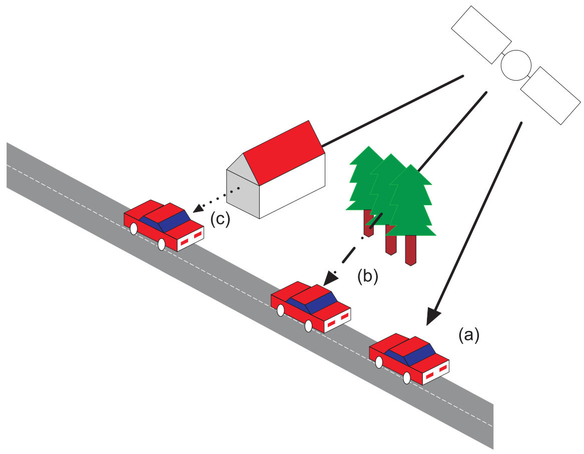

Figure 1. Direct signal power variations (slow fading) occur due to varying shadowing conditions between the satellite and a mobile receiver. They can be classified into Line-of-Sight (a), shadowed by foliage (b), or blocked by obstacles (c). This slow fading is superimposed by fast signal variations due to multipath propagation.

To derive those states from signal measurements faces two main issues: First, it requires a high transmit power satellite already in orbit. Alternatively, the satellite may have to be emulated by a helicopter equipped with a transmitter.
Second, these measurements represent only one possible realization of the satellite position in azimuth and elevation. The evaluation of modern transmission modes incorporating multi-satellite diversity (angle diversity)

needs several satellites available to be measured simultaneously. Recently, such measurements have been undertaken using the SDARS system in the U.S. [10].

A promising alternative of characterizing the LMS channel is an optical analysis of the environment. This method known as *photogrammetric satellite service prediction (PSSP)* and was introduced by Akturan *et al.* in 1994 [11]. The environment is photographed by a camera, equipped with a fisheye lens, covering the upper hemisphere. Subsequently, the channel states are derived by image processing and pattern recognition techniques [12].

The optical approach is particularly promising at higher frequency bands such as Ku or Ka band. In fact, here mostly high gain antennas are applied and the impact of multipath propagation can be neglected.
Consequently the information about LoS (Line-of-Sight) or NLoS (Non-Line-of-Sight) condition is sufficient for the modeling of the different channel states.
In combination with the models for atmospheric effects at this frequency bands such as ITU-R P.618-1 (see [13]) a realistic LMS channel model can be derived. Measuring the LMS channel is quite challenging as a perfect tracking of the high gain antenna has to be assumed.

In [14], the satellites visibility was compared with the measured power levels, already.
The present contribution is about the extraction of the satellite reception states from images. The evaluation of this approach is performed from the statistical channel modeling point of view. To verify the accuracy of our results, we compare them with results based on measured power levels, as a reference. This paper is organized as follows: Section 2 describes the measurement validation campaign and data analysis. Subsequently, in Section 3 the statistics of the measured RF signal and the optical channel conditions are compared. Finally, Section 4 concludes the paper.

2. MEASUREMENTS AND DATA ANALYSIS

2.1. Data Acquisition

Extensive measurements in the S-band were conducted in the context of the project Mobile satellite channeL with Angle DiversitY (MiLADY) [10].

In Figure 2, the traveled distance of 3700 km along the east coast of the U.S. is shown. The measurement equipment synchronously recorded the received power levels of Sirius XM Radio, operating in the S-band at 2.3 GHz. This system consists of two geostationary (GEO) satellites and three highly elliptical orbit (HEO) satellites, where two of the three HEOs were always visible at the same time. The sampling rate of the power levels was 2.1 kHz. The exact measuring time and vehicle position was logged via GPS. Moreover, two cameras were

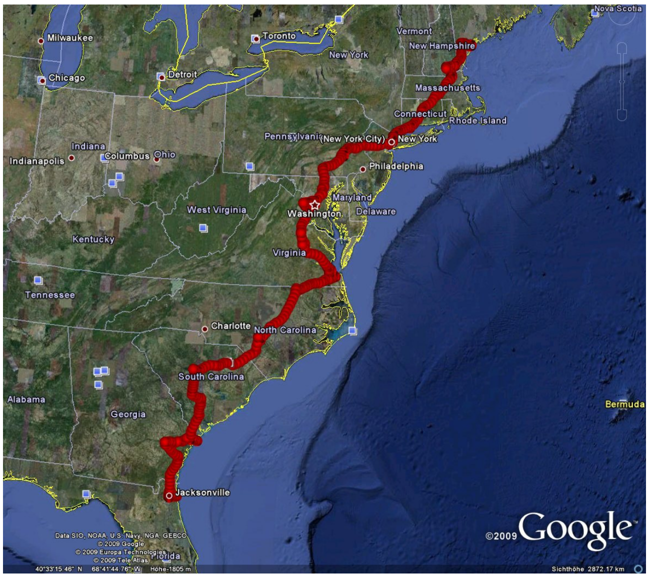

Figure 2. Measurement campaign of about 3700 km along the east US coast.

mounted on the van to document the environmental conditions. The upper hemisphere was captured by JPEG-compressed color images with a frame rate of about 5 frames per second and a resolution of 1024×768 pixels. Some regions near the horizon were not covered by the camera.

2.2. Image Processing and Analysis

In this contribution we want to derive the LMS channel reception state from images of the environment.
First of all, the hemispheric images were classified into *Sky* and *Object*. A robust image analysis technique was applied using a color clustering approach in the RGB color space. A possible implementation that models the color distributions of the classes as multivariate Gaussians and estimates the class parameters via the Expectation Maximization (EM) algorithm, is described in [15]. A result of this binary classification is depicted in Figure 3. The sun drives the camera sensor into saturation and marks a black dot in the images.

In a second step, the conversion from the classified fisheye images to rectangular images in landscape panoramic form was performed. The transformation is processed such that the output panoramic image is represented of a polar coordinate system, as you can see in Figure 4. Thus, objects appear less distorted.
Additionally, the images are shifted based on the GPS heading information of the car, thus $0°$ corresponds to the north direction.
Consequently, it is possible to choose any position in elevation and azimuth for arbitrary satellite constellations. By fusing the time- and location-information we determine the satellite positions in the binary images. The

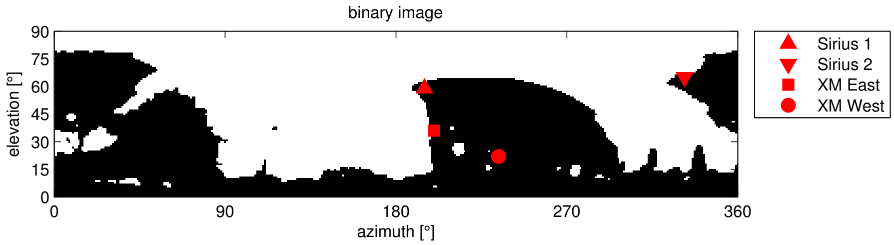

Figure 4. The hemispheric images are converted to panoramic binary images. They are of the size 91×360 pixels, where the resolution is one degree in elevation and in azimuth. The symbols show the four satellites (Sirius 1, Sirius 2, XM East and XM West) at their position.

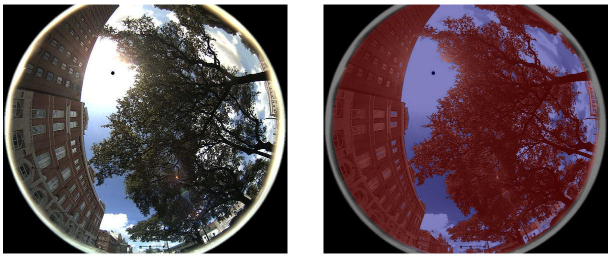

Figure 3. The shadowing conditions between the satellite and the mobile receiver are examined using a hemispheric camera. The images show an exemplary hemispheric image (left) and the overlay of the binary classification into Sky and Object (right).

symbols (▲, ▼, ■, ●) represent the four different satellites: Sirius 1, Sirius 2, XM East and XM West.

The panoramic image can be used to derive the reception state of the satellites, which is necessary for LMS channel modeling (Section 2.3).

2.3. State Modeling and State Identification

We characterize the LMS channel on the basis of a sequence of reception states consisting of (*good* and *bad*), corresponding to the reception status *LoS / light shadowing* and *NLoS / heavy shadowing*, respectively [8, 9]. In order to validate our approach, we compare state sequences derived from images with states derived from RF signals.

For state detection from RF data, first the recorded satellite power levels are normalized to the LoS level [16]. Afterwards, the states are found by global thresholding of 5 dB below LoS, which is performed on the low-pass filtered signal (same procedure as in [17, 18]).
To derive state sequences from image data, the binary value from the panoramic image at a defined satellite position is taken, where white represents the *good* state and black the *bad* state.

3. RESULTS

A preliminary comparison between RF and image state sequences in this paper is performed for one hour of measurements in the area of Portland (urban / suburban). In Figure 6 the actual RF signal levels (blue solid line) and the corresponding binary image values (red circles) are compared as time series. Each satellite signal (Sirius 1, Sirius 2, XM East and XM West) is plotted in a separate diagram, over a time period of approximately 2 min.
From the slow fading point of view, the binary values and the RF signal level are clearly in good agreement. Nevertheless, there are some parts which do not fit, such as in the first diagram from 15:01:07 till 15:01:15. Indeed, in this case the satellite position was at the edge of a building, which can cause erroneous identifications. Other possible reasons are e.g. windows in which the sky is mirrored and consequently they are incorrectly detected as sky.

Table 1 shows the correlation factor $r(x, y)$ between the state sequence from RF x and from images y, both of the length N. It is defined as

$$r(x, y) = \frac{1}{N} \sum_{x_i = y_i} 1 \quad \text{for } \mathrm{i} = 1, .., \mathrm{N}. \qquad (1)$$

x and y are $\in \{0, 1\}$, where “0” represents the *bad* state and “1” the *good*.
For all satellites a high (0.83 to 0.95) correlation is obtained. There is a clear tendency of an increasing correlation $r(x, y)$ associated with an increasing mean elevation angle ϕ.
At high elevation angles (Sirius 1, Sirius 2) a clear LoS state is more probable. This leads to a more successful state identification, as shown by the higher correlation coefficient (0.91 and 0.95).

Table 1. Mean elevation angle ϕ for the different satellites. For each, the correlation factor $r(x, y)$ between the state sequence of RF x and image data y is obtained.

	Sirius 1	Sirius 2	XM East	XM West
ϕ	65°	68°	38°	23°
$r(x, y)$	0.91	0.95	0.84	0.83

For lower elevations, as (XM East, XM West) at 38°, false detected windows and building edges are a problems to cope with (referring to Section 2.2).

From the LMS channel modeling point of view, several statistical parameters need to be determined. Therefore, the evaluation is carried out in terms of state probabilities and state duration statistics.
In Figure 5 are plotted the calculated *good* state probability for Sirius 1, Sirius 2, XM East and XM West, comparing the results of the RF and image based analysis.

Since only two states are assumed, the *bad* state probability is calculated using $P_{\text{bad}} = 1 - P_{\text{good}}$.
Obviously, the *good* state probability is greater for HEO satellites (Sirius 1, Sirius 2), because of the higher elevation angles (see Table1). Their probabilities are between 0.94 and 0.87, thereby RF and image data correspond very well.
For lower elevations (XM East, XM West) the state probability is 0.77 and 0.57. The probabilities for RF and image fit very well, only with slight deviations between 0.03 and 0.07.
Generally, the image-based *good* state probability is lower due to the fact that the binary image only distinguishes between clear LoS and everything which is left over. In comparison, the thresholding of the RF signal level at 5 dB below LoS corresponds more to the meaning *LoS/ light shadowing* and *NLoS/ heavy shadowing*.

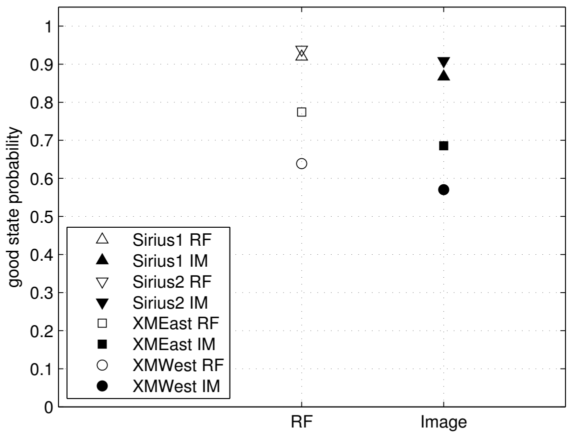

Figure 5. The good state probability for each satellite, comparing the states derived from RF signal levels and binary image values.

The state duration statistics are presented in four diagrams, each related to one satellite, all shown in Figure 7. In order to evaluate and analyze the matching of the generated RF and image states, we used the complementary cumulative distribution function. Comparing the different satellites, the *good* state durations are on average greater for Sirius 1 and Sirius 2 because of their higher elevation angle. Both GEO satellites (XM West, XM East) have an almost equal probability distribution function for *good* and *bad* state. With respect to RF based states and images based states the functions match very well for *good* , only with slight differences ($\leq 1\,\text{sec}$) . The *bad* state duration statistics show a higher deviation up to $2\,\text{sec}$ (at $P = 0.4$), however the tendency of the curves is similar.

4. CONCLUSIONS

In this paper, we jointly analyzed the measured RF signal level of various satellites with the binary value corresponding to the satellites, obtained from unwrapped panoramic images (originally hemispheric images). Furthermore, we determined reception states to characterize the propagation channel. The RF and images based states present a high correlation. As a further evaluation criterion, the RF and image state probabilities and the state duration statistics are compared.
The statistical parameters are fairly matching, especially for satellite positions with high elevation angle. It is found that slow-fading effects (states) due to signal blockages can be reliably detected by the optical method. For fast signal variations, statistical models (cf. Loo's distribution [3]) would offer a complement. From this we can conclude that the image based state reception in combination with e.g. a Loo parameter estimation is a reliable multi-satellite modeling method. Nevertheless, some improvement can be carried out by coping with false detected windows, edges of buildings and overexposure.

In particular, the presented approach works even more correctly for higher frequency bands as Ku and Ka, where shadowing and obstruction play a decisive role. Due to the high directivity of the antennas employed, the channel is similar to an optical channel. For the future a hybrid model, including also the atmospheric effects, could be possible, as their effects are uncorrelated. In combination with the models for atmospheric effects at this frequency bands, such as ITU-R P.618-1 ([13]), a realistic LMS channel model could be derived.

ACKNOWLEDGMENT

The measurements were carried out in the context of the project MiLADY (Mobile satellite channeL with Angle DiversitY), funded by the European Space Agency (ESA) under contract number C21150.

REFERENCES

[1] Riza Akturan. An overview of the Sirius satellite radio system. *International Journal of Satellite Communications and Networking*, 26(5):349–358, 2008.

[2] Richard A. Michalski. An overview of the XM satellite radio system. In *20th AIAA International Communication Satellite Systems Conference and Exhibit*, May 2002.

[3] Chun Loo. A statistical model for a land mobile satellite link. *IEEE Transactions on Vehicular Technology*, 34(3):122–127, August 1985.

[4] Erich Lutz, Daniel Cygan, Michael Dippold, Frank Dolainsky, and Wolfgang Papke. The land mobile satellite communication channel – recording, statistics, and channel model. *IEEE Transactions on Vehicular Technology*, 40(2):375–386, 1991.

[5] Wolfhard J. Vogel and Julius Goldhirsch. Multipath fading at L band for low elevation angle, land mobile satellite scenarios. *IEEE Journal on Selected Areas in Communications*, 13(2):40–76, February 1995.

[6] Fernando Pérez-Fontán, Maryan Vázquez-Castro, Cristina Enjamio Cabado, Jorge Pita García, and Erwin Kubista. Statistical modeling of the LMS channel. *IEEE Transactions on Vehicular Technology*, 50(6):1549–1567, November 2001.

[7] Fernando Pérez-Fontán, Maria Angeles Vázquez-Castro, C. Enjamino, and Jorge Pita García. Comparison of generative statistical models for the LMS channel. In *IEEE 55th Vehicular Technology Conference, VTC Spring 2002*, volume 2, pages 871–875, 2002.

[8] R. Prieto-Cerdeira, F. Perez-Fontan, P. Burzigotti, A. Bolea-Alamañac, and I. Sanchez-Lago. Versatile two-state land mobile satellite channel model with first application to DVB-SH analysis. *International Journal of Satellite Communications and Networking*, 28(5-6):291–315, 2010.

[9] Erich Lutz. A Markov model for correlated land mobile satellite channels. *International Journal of Satellite Communications*, 14:333–339, 1996.

[10] Ernst Eberlein, Albert Heuberger, and Thomas Heyn. Channel models for systems with angle diversity – The MiLADY project. In *ESA Workshop on Radiowave Propagation Models, Tools and Data for Space Systems*, Noordwijk, the Netherlands, December 2008.

[11] Riza Akturan and Wolfhard J. Vogel. Photogrammetric mobile satellite service prediction. In *Proceedings of the Eighteenth NASA Propagation Experimenters Meeting (NAPEX XVIII) and the Advanced Communications Technology Satellite (ACTS) Propagation Studies Miniworkshop*, pages 159–163, Vancouver, BC Canada, June 1994.

[12] Hsin-Piao Lin and Wolfhard J. Vogel. Photogrammetric satellite service prediction in a roadside tree-shadowing environment. In *Vehicular Technology Conference*, volume 2, pages 1485–1487, 1998.

[13] ITU-R. Propagation data and prediction methods required for the design of earth-space telecommunication systems. *Rec. ITU-R P.618-10*, 2010.

[14] A. Ihlow, D. Arndt, F. Topf, C. Rothaug, T. Wittenberg, and A. Heuberger. Photogrammetric satellite service prediction-correlation of rf measurements and image data. In *Broadband Multimedia Systems and Broadcasting (BMSB), 2011 IEEE International Symposium on*, pages 1–6. IEEE, 2011.

[15] Alexander Ihlow and Albert Heuberger. Sky detection in fisheye images for photogrammetric analysis of the land mobile satellite channel. In *Proceedings of the 10th Workshop Digital Broadcasting*, pages 56–60, Ilmenau, Germany, September 2009.

[16] Daniel Arndt, Alexander Ihlow, Albert Heuberger, Thomas Heyn, and Ernst Eberlein. Land mobile satellite channel characteristics from the MiLADY project. In *Proceedings of the 10th Workshop Digital Broadcasting*, pages 49–55, Ilmenau, Germany, September 2009.

[17] L.E. Braten and T. Tjelta. Semi-markov multistate modeling of the land mobile propagation channel for geostationary satellites. *Antennas and Propagation, IEEE Transactions on*, 50(12):1795–1802, 2002.

[18] D. Arndt, A. Ihlow, T. Heyn, A. Heuberger, R. Prieto-Cerdeira, and E. Eberlein. State modelling of the land mobile propagation channel for dual-satellite systems. *EURASIP Journal on Wireless Communications and Networking*, 2012(1):228, 2012.

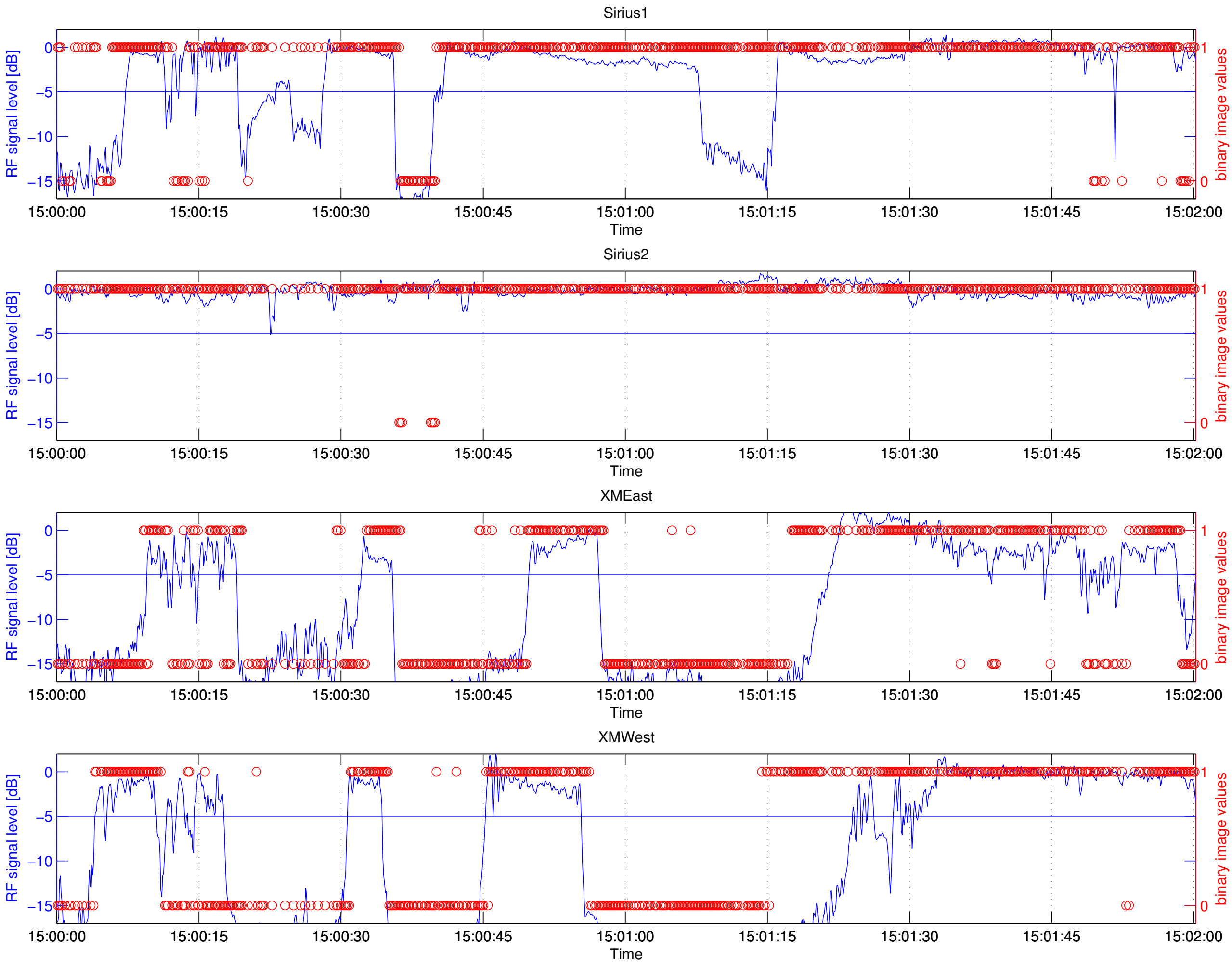

Figure 6. The measured RF signal level (blue) and the corresponding binary values (red circles) are plotted for each of the four satellites (Sirius 1, Sirius 2, XM East and XM West) over a certain time period (≈ $2\,\mathrm{min}$). The horizontal line shows the threshold for state identification, which is 5dB below the LoS.

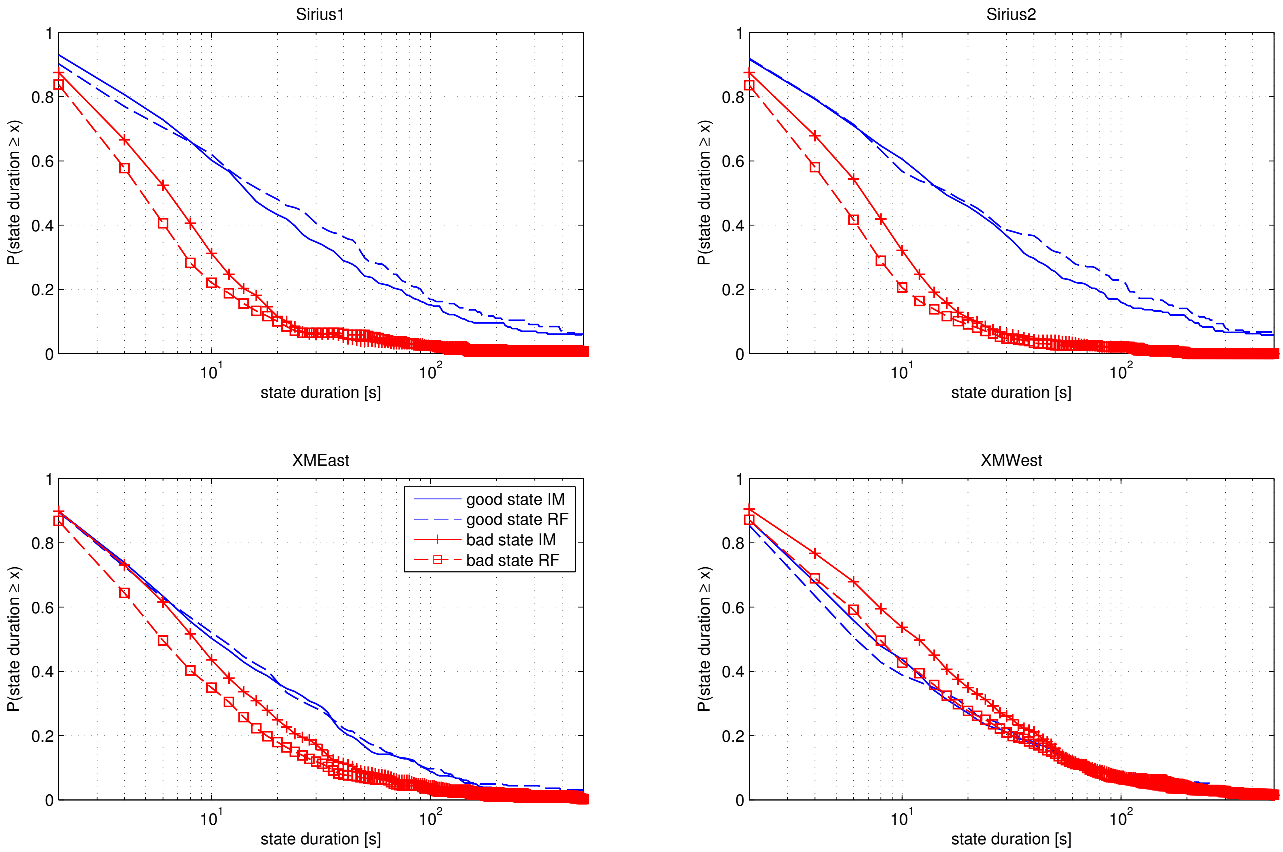

Figure 7. State duration statistics for good (blue) and bad (red) state are presented for each satellite (Sirius 1, Sirius 2, XM East and XM West). Additionally, they are analyzed for RF based states (dashed lines) and image (IM) based states (solid lines).